Quantum Electronics **50** (12) 1160–1166 (2020)

LASER APPLICATIONS AND OTHER ISSUES IN QUANTUM ELECTRONICS https://doi.org/10.1070/QEL17404

Statistical characteristics of laser interference and its effect on IR optoelectronic observation systems

N.I. Pavlov, Yu.A. Rezunkov

Abstract. **We consider statistical characteristics of laser interference recorded in the focal region of an IR optoelectronic observation system under field and out-of-field illumination by laser radiation. The applicability of the analytical description of experimental histograms of the laser interference signal distribution at the photodetector array output using the probability density approximations in the form of gamma distribution and the Gaussian function is substantiated. It is shown that the specific form of these functions is determined both by the mean value (mathematical expectation) of the interference signal and by the characteristic parameter *M*, which depends on the statistical properties of the laser interference.**

Keywords: *IR optoelectronic system, quasi-point object, laser interference, probability density distribution, gamma distribution, Gaussian function, false alarm probability, probability of missing a target.*

1. Introduction

Laser irradiation of optoelectronic systems (OES's) for observing quasi-point objects (targets) is an urgent problem that has drawn considerable attention of specialists [1–6]. It is known that the effects of laser radiation are most strong if the laser irradiates the OES within the system's sensitivity spectral range. In real conditions, two main regimes of laser impact can be implemented: the field impact when the laser source is located in the optical system's field of view and its radiation is focused on the photodetector array, and the out-of-field impact, when the laser source is located outside the optical system's field of view and the photosensitive array is illuminated by radiation scattered on optical and structural elements of the receiving objective.

Analysis of experimental studies from [2–6] shows that the field impact forms a region of 'saturated' pixels in the focal photodetector array (FPDA) (a region of the laser beam core), outside of which the laser radiation intensity decreases quite rapidly with distance from the core. This change in the radiation intensity makes it possible to estimate it using an analytical approximation of the point spread function of the receiving objective. It should be noted that the saturation intensity of photosensitive FPDA elements depends on the laser radiation, which can be either pulsed or continuous. An increase in the radiation power can lead to the destruction of the photodetector's sensitive elements located in the laser beam's core region or adjacent to it.

Description of the results of out-of-field laser impact on the OES, caused by the illumination of the photodetector array by scattered radiation (hereinafter referred to as laser interference), is a more complicated problem. Experimental studies performed in work [1] show that the distribution of the scattered radiation intensity in the array photodetector plane has a speckled character. In this case, the scattered radiation recorded by the FPDA is perceived as an additional noise signal that reduces the OES detection capabilities. For OES observation of quasi-point objects (we consider IR systems below), the probabilities of a false alarm and missing a target are usually considered as detection characteristics using Gaussian approximations of the intensity of real background illumination. It follows from the results of work [1] that laser interference cannot be described by a Gaussian probability density distribution. In this regard, the determination of its effect on the specified OES detection characteristics requires separate consideration, which is the subject of this paper.

The theoretical study conducted in this work is based both on experimental data obtained earlier [1, 2] and on a number of additional experiments on irradiating the OES prototype by radiation from pulsed CO and HF lasers. The result of this theoretical analysis is an analytical method for evaluating the detection characteristics of the investigated (projected) OES, developed on the basis of studies on the statistical characteristics of laser interference in the conditions of FPDA illumination by scattered laser radiation. The proposed method uses both gamma distribution [7] and Gaussian approximation [8] to describe the probability density distribution of the interference signal as a function of the mean value $\bar{U}$ of the recorded laser interference voltage at the FPDA output and the characteristic parameter M that depends on the coherent properties of the scattered laser radiation incident on the focal array. Implementation of the method implies the need to design a prototype of the investigated OES for conducting experiments in order to obtain data on the specified statistical characteristics of laser interference.

Note that in works [1, 2] an OES prototype was used, the optical system of which was an objective based on an off-axis parabolic mirror with a hood, while a cooled array with InSb sensitive elements of 128×128 pixels served as a photodetector. The theoretical analysis performed in this paper is extended to cases when laser interference caused by scattered laser radiation is recorded by a focal array in the linear range of its sensitivity.

N.I. Pavlov, Yu.A. Rezunkov Scientific Research Institute for Optoelectronic Instrument Engineering, Leningradskaya ul. 29, 188540 Sosnovyi Bor, litera T, Leningrad region, Russia; e-mail: yuri@sbor.net

Received 15 June 2020
Kvantovaya Elektronika **50** (12) 1160–1166 (2020)
Translated by M.A. Monastyrskiy

2. Features of the formation of laser interference by scattered radiation: analysis of experimental data

Experimental studies [1, 2], conducted with the participation of one of the authors of this work, show that there are general regularities in the laser interference formation both in the field and out-of-field effects on the OES, which consist in the formation of a speckled light field in the focal region of the optical system.

Under the field impact, a complex pattern of the radiation intensity distribution recorded by the focal FPDA is formed (Fig. 1 a). The region of the laser beam core, i. e. the region of saturated pixels, is surrounded by a region of functionally suppressed pixels, where the radiation intensity decreases quite rapidly with distance from the core. Radiation scattered on technological roughness of surfaces in the system's optical elements, which has the form of a speckled image when recorded, makes a significant contribution to the irradiation of the FPDA surface region located outside the core [1–4].

The exact shape of the FPDA signal distribution under field impact depends on many factors determined by the specific optical system of the OES. For its approximate estimation, various analytical approximations of the point spread function (PSF) of the receiving objective are used. In particular, a PSF approximation was proposed in work [3] in the form of a function of the distance from the centre of the laser beam core:

$$\mathrm{PSF}(x) \approx (1-\rho)\frac{4}{\pi x^3 + 4} + \rho.$$

Here, an attempt is made to take into account the effect on the PSF of radiation scattering on optical elements through a small parameter ρ, which characterise the scattering intensity when the OES is irradiated with laser light.

The radiation intensity during out-of-field exposure primarily depends on the illumination angle θ (the angle between the laser beam axis and the optical axis of the receiving objective) of the OES optical system. A characteristic feature of laser interference in this case is a speckled distribution of the light field intensity, i. e., a quasi-regular intensity distribution with a certain spatial scale and amplitude. An example of such a speckle signal is shown in Fig. 1 b, where an image of laser interference is shown together with a signal from a target simulator in the form of a bright horizontal band, recorded during out-of-field illumination of the OES prototype [1] by HF laser radiation. At a certain radiation intensity, laser interference completely suppresses the signal from the target.

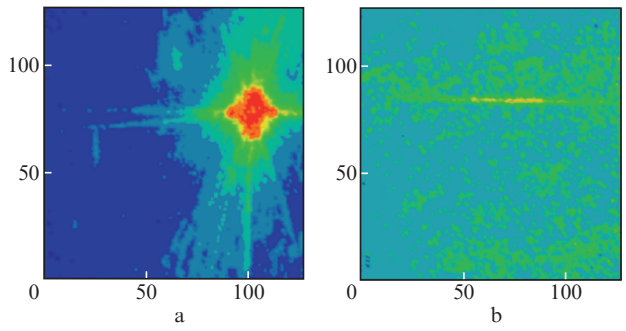

Figure 1. (Colour online) Examples of (a) field and (b) out-of-field effects on images recorded by the FPDA with a signal from the target simulator in the form of a bright horizontal band. Here and in Figs 2 and 4 the digits on the axes are the column and row numbers of the OES receiver FPDA.

As was first shown in work [1], the distribution of laser interference signals over FPDA pixels depends on the spectral composition and polarisation of the laser radiation. In turn, the spectral composition of radiation is determined by its characteristics such as temporal and spatial coherence. In conditions when an inhomogeneous radiation distribution with integration of instantaneous intensity over a finite time is recorded using the FPDA, the degree of coherence affects the root mean square value of the ratio of the recorded signal to its noise [7]. From a physical point of view, this value depends on the ratio between the time of signal accumulation in the FPDA and the coherence time of the radiation forming this signal. In this case, assuming that speckled laser radiation is ergodic and statistically stationary during signal accumulation, we use the gamma distribution to describe histograms of signal distributions in the laser interference images recorded by the FPDA. The characteristic parameter included in the function describing this distribution is the parameter M, which depends on both the spectral characteristics of laser radiation and the optical parameters of the OES.

For the speckle structure of partially polarised radiation, formed as a sum of two independent light fields (fully polarised and fully depolarised scattered radiation), the probability density function (PDF) of the radiation intensity distribution has the form [7]

$$\mathrm{PDF} = \frac{\sqrt{\pi}}{\Gamma(M)}\left(\frac{Mu}{P\bar{U}}\right)^M \left[\frac{4PM}{(1-P^2)u\bar{U}}\right]^{1/2} \times \exp\left[-\frac{2Mu}{(1-P^2)\bar{U}}\right] I_{M-1/2}\left(\frac{2PM}{(1-P^2)\bar{U}}\right), \quad (1)$$

where $I_{M-1/2}$ is the modified Bessel function of the 1st kind of order $M-1/2$; $\Gamma(M)$ is the gamma function of the parameter M; P is the radiation polarisation degree; and u is the current value of the signal from the array's pixels (in volts).

In the case of fully developed speckles and fully depolarised radiation, the PDF function appears as [7]:

$$\mathrm{PDF}(P=0) = \left(\frac{2M}{\bar{U}}\right)^{2M} \frac{u^{2M-1}}{\Gamma(2M)} \exp\left(-2M\frac{u}{\bar{U}}\right). \quad (2)$$

The relation of the parameter M with the mean value of the recorded interference signal voltage determined from the experiment (mathematical expectation $\bar{U}$) and the corresponding root-mean-square value σ_{sn} up to a constant multiplier $(1+P^2)^{1/2}$ is described by the expression [7]

$$\sigma_{\mathrm{sn}} = \sqrt{1/(2M)}\,\bar{U}. \quad (3)$$

It is known (see, for example, [9]) that the polarisation of laser radiation after reflection from the structural elements and optical elements of the receiving objective in the OES depends on the material from which these elements are made, and the illumination angle θ. Multiple reflections of laser radiation lead to its almost complete depolarisation. As shown in work [1], the polarisation degree P of laser radiation in the focal region of the objective in the OES prototype was 0.58 at $\theta = 2°$ and decreased with increasing θ due to multiple reflections of scattered radiation.

We determine the specific shape of the PDF function from experimental frames of laser interference recording obtained using relation (3) and the sequence of operations described in work [1]. As an example, Fig. 2 shows images of the laser interference signal under the field-type effect of pulsed CO and HF laser radiation on the OES model. Areas highlighted in white correspond to the saturated pixels of the array. Figure 3 shows the histograms of the laser interference signal distributions based on these images. When constructing approximations of experimental histograms of the laser interference signal distribution (blue curves) and analytical approximations of these histograms by the PDF function having form (2) (red curves), the white image areas were not taken into account. The integral (area under the PDF curve) of the signal's probability density distribution is equal to unity. The parameter M in expression (2) is 3.0 when exposed to a CO laser and 2.1 when exposed to an HF laser. These values are quite close.

Examples of experimental images of a laser interference signal under an out-of-field impact ($\theta = 2°$) on the OES prototype with the 2nd harmonic of CO_2 laser radiation, taken from [1], are shown in Fig. 4 for the radiation coherence lengths l_{coh} = 3 and 0.003 m. Histograms of the interference signal distribution (circles corresponding to the vertices of rectangles) and their approximations using the PDF function (2) (solid curves) and the Gaussian function [see (8) below]) (dashed curves) are shown in Fig. 5. The parameter M values in this case are already significantly different: M = 4.20 at l_{coh} = 3 m and M = 9.61 at l_{coh} = 0.003 m.

The presented results show a fairly good agreement between the experimental distributions of the laser interference signal and their approximation by the PDF function (2) (hereinafter referred to as the gamma distribution) when using relation (3) for both field and out-of-field irradiation of the OES prototype. It is also obvious that the parameter M depends on the laser radiation's spectral characteristics and on the regime of laser irradiation of the OES (field or out-of-field). Additional analysis has shown that the parameter M varies from 1 to 3 for field exposure, and from 3 to several tens for out-of-field exposure, depending on the illumination angle of the OES receiving objective, i.e., with increasing exposure angle, the contribution of multiple radiation reflections to the laser interference signal increases, which reduces its coherence degree.

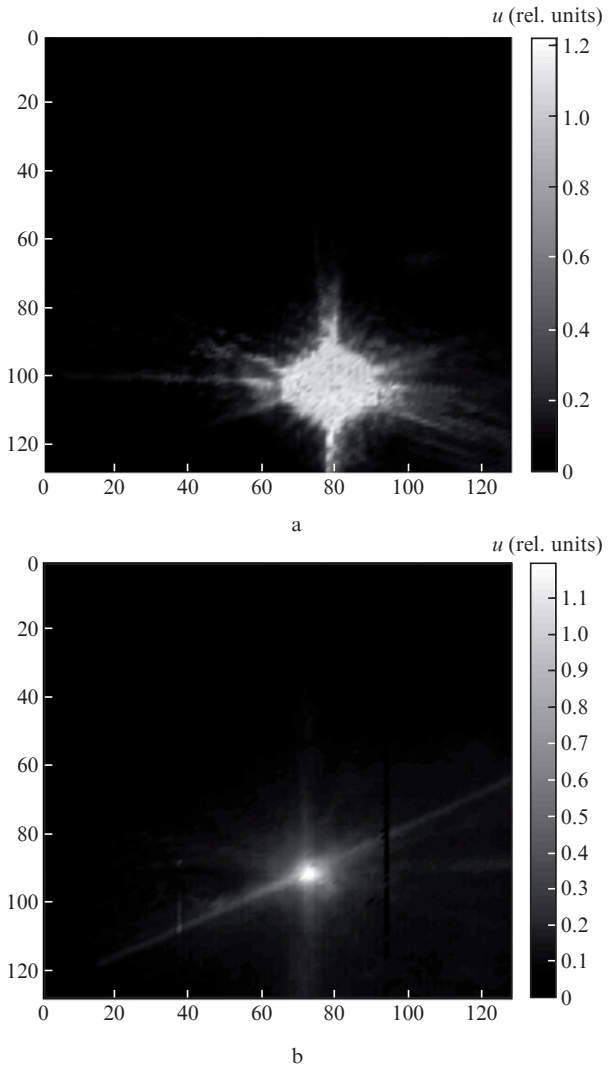

Figure 2. Images of the laser interference signal under the field impact on the OES prototype of (a) CO and (b) HF laser radiation.

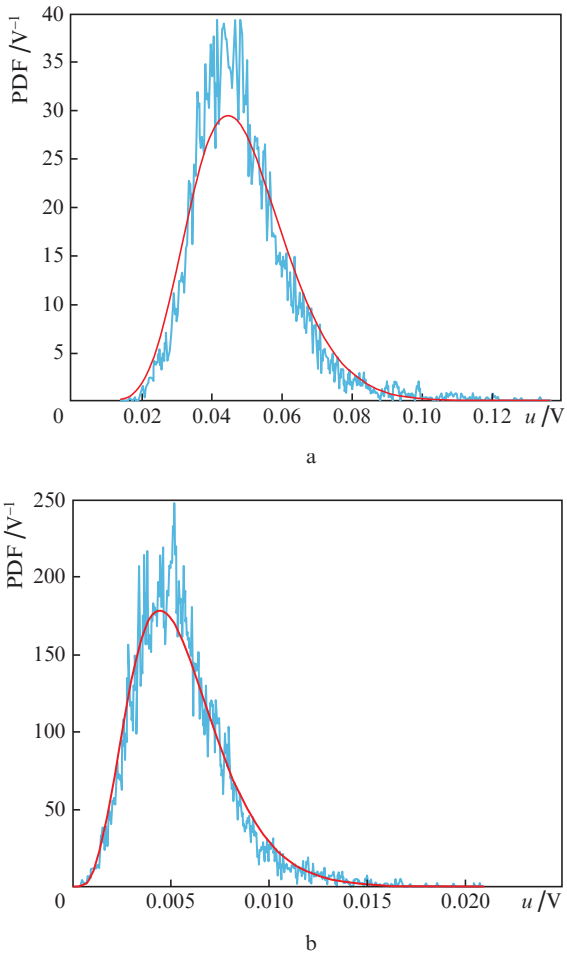

Figure 3. (Colour online) Distribution histograms of the laser interference signal (blue curves) and their approximations by function (2) (red curves) when the OES prototype is exposed to radiation from (a) CO and (b) HF lasers for M = (a) 3.0 and (b) 2.1.

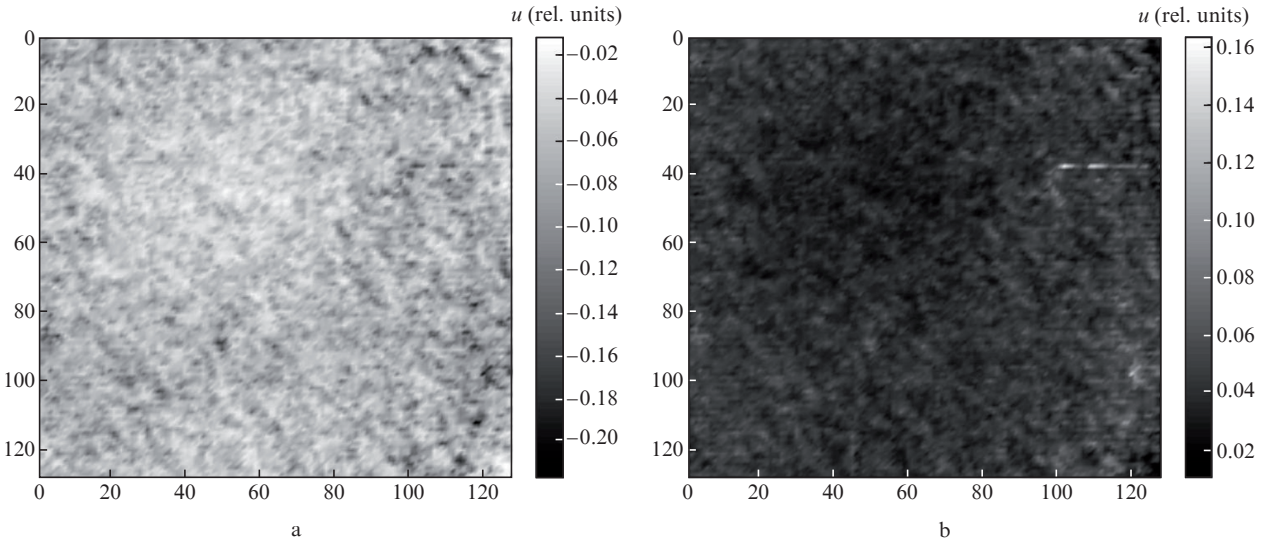

Figure 4. Images of the laser interference signal obtained during out-of-field exposure ($\theta = 2°$) of the OES prototype to radiation from the second harmonic of a CO_2 laser for l_{coh} = (a) 3 and (b) 0.003 m.

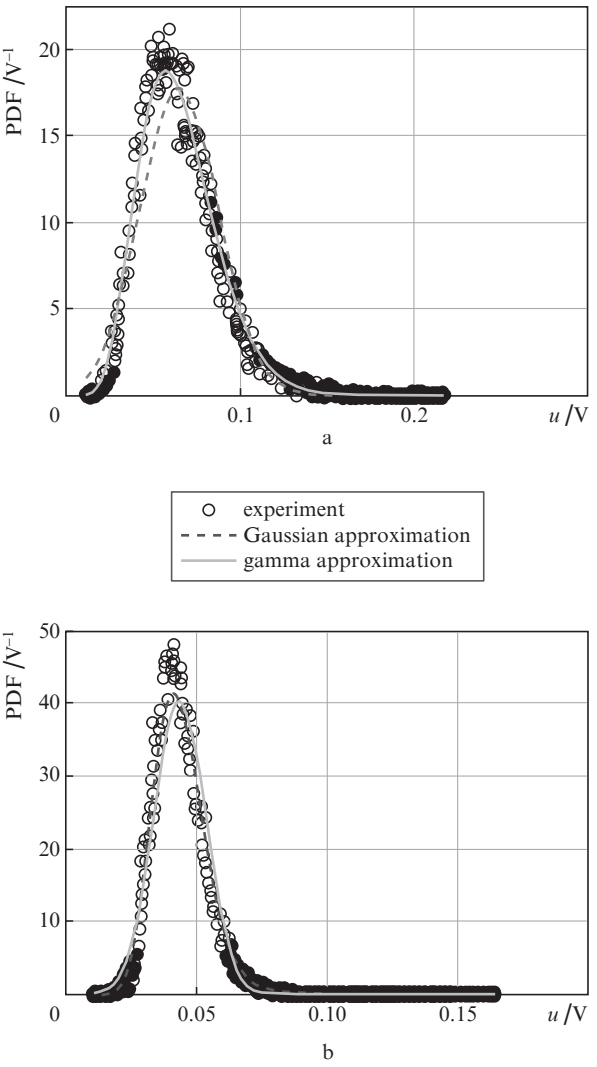

Figure 5. Gamma approximation and Gaussian approximation of the laser interference signal for (a) l_{coh} = 3 m, M = 4.20 and (b) l_{coh} = 0.003 m, M = 9.61.

3. Laser interference impact on the probability of false alarm and missing a target

The functional capabilities of optoelectronic detection systems are most commonly established using statistical characteristics such as the probability of false alarm (implementation of the alternative hypothesis is determined by the probability of correct non-detection) and the probability of missing a target (implementation of the alternative hypothesis is determined by the probability of correct detection). Various optimal detection criteria are used to find the threshold voltage U_{th} for triggering the detection device. In practice, the Neumann–Pearson criterion is preferable, since it does not require knowledge of *a priori* probabilities and, in the case of a Gaussian signal distribution, provides the maximum probability of correct detection of a quasi-point object for a given false alarm probability [8, 10]. The analysis below is an analytical description of the probabilities of false alarm and missing a target during laser impact on the OES, with justification for the approximation of the laser interference signal by both the Gaussian function and the gamma distribution.

In all the considered cases, in order to exclude the effect of the natural laboratory background and to take into account only the effect of laser interference on the OES detection characteristics, the pre-formed background image was subtracted from the working image with laser interference [1]. In this case, the residual (unavoidable) root-mean-square value of the intrinsic noise voltage of the array σ_n did not exceed 0.002 V at a signal accumulation time of 100 μs. In the absence of laser interference, the signal-to-noise ratio SNR = $U_s/\sigma_n \geqslant 20$, which guaranteed close-to-unity values of the signal detection probability P_d with a probability of a false alarm $P_{fa} \leqslant 0.001$. To ensure $P_{fa} = 0.001$, we have chosen $U_{th} = 0.012$ V. Below in this paper, these initial values are used to theoretically study the effect of laser interference on the OES detection characteristics.

An estimate of the false alarm probability can be obtained using the expression [8]:

$$P_{fa} = \int_{U_{th}}^{\infty} \mathrm{PDF}(u)\,\mathrm{d}u, \qquad (4)$$

where PDF is the probability density function of the interference signal distribution. In the case of laser interference, expression (4) for the false alarm probability, with allowance for (2), transforms to the form

$$P_{\text{fa}} = \int_{U_{\text{th}}}^{\infty} \frac{(2M)^{2M}}{\bar{U}^{2M}} \frac{u^{2M-1}}{\Gamma(2M)} \exp\left(-2M\frac{u}{\bar{U}}\right) \mathrm{d}u$$
$$= \frac{(2M)^{2M}}{\Gamma(2M)} \int_{U_{\text{th}}/\bar{U}}^{\infty} z^{2M-1} \exp(-2Mz)\,\mathrm{d}z\,, \qquad (5)$$

i.e., the probability P_{fa} depends both on the mean value of the laser interference voltage $\bar{U}$ and on the coherence of the generated light speckle field, which is generally determined by the characteristic parameter M.

As an illustration of this dependence, Table 1 shows the estimates of the false alarm probability, calculated by formula (5) with the field exposure of the OES prototype to pulses of two types of lasers, whose energies are different. The parameter M was determined from the experimentally measured mean ($\bar{U}$) and root-mean-square (σ_{sn}) values of the interference signal in accordance with expression (3). These lasers are characterised by the multispectrality of the generated radiation (up to 10 spectral lines per pulse) and, as a consequence, a low degree of radiation coherence.

Table 1. Probabilities of a false alarm and missing a target in multispectral laser irradiation of the OES prototype.

Laser type	σ_{sn}/V	$\bar{U}$/V	M	P_{fa} (5)	P_{fa} (9)	P_{m} (12)
HF laser	0.0025	0.0037	2.19	0.0094	1.44×10^{-6}	0
	0.0055	0.0073	1.76	0.1671	0.1127	8.75×10^{-4}
	0.0555	0.0954	2.95	0.9928	0.9832	0.2943
CO laser	0.0207	0.0297	2.05	0.8872	0.8121	0.0736
	0.0678	0.0934	1.90	0.9679	0.9553	0.329

Noteworthy is the fact that the false alarm probability significantly increases with an increase in the mean and root-mean-square values of the interference signal. In this case, the parameter M for both types of lasers changes insignificantly, remaining in the range from 1.90 to 2.95.

To determine the probability of missing a target under laser interference conditions, it is necessary to know the probability density distribution of the total signal from the laser interference and the target. Assuming that two random variables (the target signal and the laser interference sign al) are independent of each other, we use the following expression for the probability density function of the total signal $f(z)$ [10]:

$$f(z) = \int_{-\infty}^{\infty} f_{\text{sn}}(z-x) f_{\text{ob}}(x)\mathrm{d}x, \qquad (6)$$

where f_{sn} and f_{ob} are the probability density distributions of the laser interference signal and the target signal, respectively. Given relation (6), the probability of missing a target P_{m} can be estimated as

$$P_{\text{m}} = \int_{-\infty}^{U_{th}} f(z)\mathrm{d}z = \int_{-\infty}^{U_{th}}\int_{-\infty}^{\infty} f_{\text{sn}}(z-x)\, f_{\text{ob}}(x)\mathrm{d}z\mathrm{d}x. \qquad (7)$$

Above, the PDF function in form (2) has been considered as the function f_{sn}. As already shown (see Figs 3 and 5), this type of PDF describes the laser interference well, including the region of large values ('spikes') of the interference signal, which is important when evaluating the false alarm probability. However, the use of PDF (2) to estimate the probability of missing a target leads to certain difficulties associated with calculating integral (7). In this regard, we consider the possibility of using the Gaussian approximation for the function $f(z)$, taking into account the proximity (within a few percent) of both theoretical distributions in the description of experimental histograms of the laser interference signal for $M \geqslant 2.0$. In this case, in both distributions, the parameter M is determined by the mean and root-mean-square values of the interference signal calculated from these histograms.

In the case of Gaussian approximation, the expression for the f_{sn} function takes the form

$$f_{\text{sn}} = \frac{1}{\sigma_{\text{sn}}\sqrt{2\pi}} \exp\left[-\frac{(u-\bar{U})^2}{2\sigma_{\text{sn}}^2}\right]$$
$$= \sqrt{\frac{M}{\pi}}\frac{1}{\bar{U}} \exp\left[-\frac{(u-\bar{U})^2}{\bar{U}^2}M\right]. \qquad (8)$$

To confirm the possibility of such an approximation, the following probability densities of the laser interference signal distribution are given in Fig. 6: experimental histogram (circles), gamma approximation by formula (2) (solid curves), and Gaussian approximation by formula (8) of the same histogram (dashed line). The experimental data in Fig. 6a were obtained by irradiating the OES prototype [1] with radiation

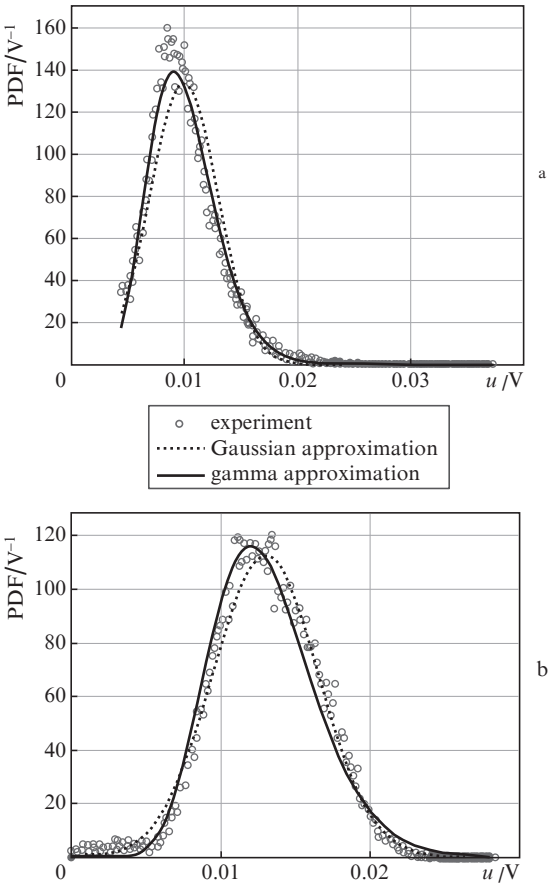

Figure 6. Probability density distributions of the laser interference signal (see text).

from a CO laser, and in Fig. 6b, with radiation from an HF laser. It was taken into account that for Fig. 6a the values of $\bar{U}$ and σ_{sn} are equal to 0.0084 V and 0.0035 V, while for Fig. 6b these values are equal to 0.0131 V and 0.0049 V, respectively. The parameter M was calculated using expression (3), as well as the experimental values σ_{sn} and $\bar{U}$.

The expression for the false alarm probability with the use of the Gaussian approximation (8) appears as

$$P_{fa} = \int_{U_{th}}^{\infty} f_{sn}(u)\,du = \frac{1}{2} - \Phi((U_{th} - \bar{U})/\sigma_{sn}), \qquad (9)$$

where

$$\Phi(x) = \frac{1}{\sqrt{2\pi}} \int_{-\infty}^{x} \exp\left(-\frac{x^2}{2}\right) dx.$$

Table 1 presents the results of calculating P_{fa} using formulas (5) and (9). It can be seen that with the Gaussian approximation (8) the false alarm probability is slightly lower (by 3%–5%) than when using PDF in form (2). Most likely, this is due to the fact that the Gaussian function gives somewhat worse description of the experimental histogram of the laser interference signal in the region of large signal spikes. Figure 7 shows the probability density distributions of the laser interference signal in the region of large signal spikes when the OES prototype is irradiated with an HF laser and the 2nd harmonic of a CO_2 laser.

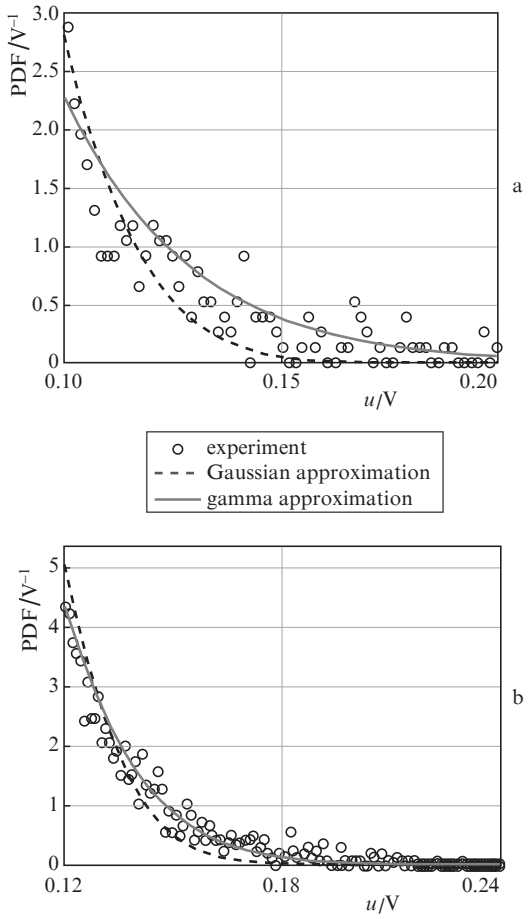

Figure 7. Probability density distributions of the laser interference signal in the region of large spikes and their approximations by the gamma distribution and the Gaussian function when the OES prototype is exposed to radiation from (a) a HF laser and (b) the 2nd harmonic of the CO_2 laser.

Below, considering the probability of missing a target, we use the Gaussian approximation (8) of the laser interference signal distribution as a function f_{sn} in expressions (6) and (7). Assuming that the signal from the target is local and deterministic, we use a model representation for f_{ob} in the form of the δ-function:

$$f_{ob}(u) = \delta(u - U_s - \bar{U}), \qquad (10)$$

which takes into account the fact of a nonzero mean value of the laser interference (stepwise), by which the useful signal U_s increases in the process of recording.

In this case, for the probability density distribution $f(z)$, we obtain the relation

$$f(z) = \frac{1}{\sqrt{2\pi}\,\sigma_{sn}} \int_{-\infty}^{\infty} \exp\left\{-\frac{[z - (u - \bar{U})]^2}{2\sigma_{sn}^2}\right\} \times \delta(u - U_s - \bar{U})\,du = \frac{1}{\sqrt{2\pi}\,\sigma_{sn}} \exp\left[-\frac{(z - U_s)^2}{2\sigma_{sn}^2}\right]. \qquad (11)$$

Given (11), for the probability of missing a target, with a signal distribution in the form of δ-function (10), we have the expression

$$P_m = \int_{-\infty}^{U_{th}} f(z)\,dz = \frac{1}{2} - \Phi\left(\frac{U_s - U_{th}}{\sigma_{sn}}\right). \qquad (12)$$

It is easy to see that the obtained expressions for the probabilities of a false alarm (9) and missing a target (12) are close to the classical ones, with the only difference that the root-mean-square value σ_{sn} of the interference signal depends on the parameter M and the mean voltage induced by the laser interference (mathematical expectation $\bar{U}$). Formula (9) also contains an additive term in the form of the induced mean voltage $\bar{U}$. The corresponding results of calculating the probability of missing a target using formula (12) are presented in Table 1, which illustrates the field effect of multispectral laser radiation on the OES prototype.

Table 2 shows the results of calculations using expressions (9) and (12) of the OES detection characteristics under laser interference conditions when the threshold voltage of the device varies. Probabilities corresponding to the same signal-to-laser interference ratio (SNR) are compared. As above, the calculations were performed using laser interference signals generated by the out-of-field impact on the OES prototype of the CO_2 laser radiation (2nd harmonic) [1]. In experiments, the signal from the target had a constant value: U_s = 0.04 V, while the mean ($\bar{U}$) and root-mean-square (σ_{sn}) values of the interference signal varied depending on the radiation power and the regime of laser exposure.

It follows from Table 2 that an attempt to reduce the false alarm probability in the presence of laser interference by increasing the detection threshold leads to an obvious result – an increase in the probability of missing a target and a decrease in the probability of its correct detection.

In the analytical expressions given above, the parameters $\bar{U}$ and M estimated from model experiments are used to calculate the functional characteristics of the OES designated for

Table 2. Signal detection characteristics against the laser interference background when the threshold voltage is varied.

U_{th}/V	SNR	P_m (12)	P_d	P_{fa} (9)
0.012	1	0.233	0.767	0.394
0.012	1.8	0.1	0.900	0.302
0.012	2.1	0.067	0.933	0.274
0.012	5.7	3.304×10^{-5}	1	0.044
0.02	1	0.291	0.709	0.326
0.02	1.8	0.175	0.825	0.193
0.02	2.1	0.136	0.864	0.159
0.02	5.7	0.002	0.998	0.002
0.03	1	0.373	0.627	0.250
0.03	1.8	0.309	0.692	0.097
0.03	2.1	0.274	0.726	0.067
0.03	5.7	0.077	0.923	9.557×10^{-6}

detecting a quasi-point observation object (target) under the action of laser interference.

4. Conclusions

The paper presents an analysis of laser impact on the detection characteristics of IR OES designated for observation of quasi-point objects (targets). The functional effect is caused by the formation of laser interference due to the scattering of laser radiation on the optical and structural elements of the OES with an FPDA. Based on the analysis, an analytical method is proposed for estimating both the false alarm probability and the probability of missing a target in the conditions of focal array illumination by scattered laser radiation. This method is based on determining the probability density function of the laser interference signal with the parameters $\bar{U}$ (the mean value of the recorded laser interference voltage at the FPDA output) and M (the parameter characterising the statistical properties of scattered laser radiation incident on the photodetector array). It is shown that the approximation of experimental histograms in the form of both the gamma distribution and the Gaussian function can be used to determine the false alarm probability. The Gaussian function is used to derive an expression for the probability of missing a target.

For an *a priori* (without conducting model experiments) prediction of the effect of laser interference on the OES detection characteristics based on the above dependences P_{fa} and P_m, it is necessary to develop computational models for the parameters $\bar{U}$ and M. The theoretical determination of the parameter $\bar{U}$ for a given laser irradiation of the entrance pupil of an optical system does not present any special difficulties, except for the calculation of the transmittance (transmission) of laser radiation to the focal plane in the process of out-of-field illumination. However, today this calculation is available for almost any optical system using a software package such as ZEMAX or a specialised program (see, for example, [11]). The parameter M depends both on the coherence degree of the laser radiation incident on the OES entrance pupil, and on the conditions for the formation of scattered radiation on the photodetector array and its conversion into voltage signals. In our opinion, the development of a mathematical model for estimating the parameter M is a more complex problem and requires a more detailed analysis of the statistical properties of speckle fields arising from the interaction of laser radiation with the OES optomechanical elements [12], which may be the subject of further research.

Acknowledgements. The authors express their gratitude to L.A. Reyankova for preparing the actual materials obtained during the processing of laser interference images recorded by the FPDA.

References

1. Asanov S.V., Ignat'ev A.B., Morozov V.V., et al. *Opt. Zh.*, **79** (9), 23 (2012).
2. Asanov S.V., Egorov M.S., Ignat'ev A.B., et al. *Opt. Zh.*, **81** (9), 62 (2014).
3. Schleijpen R.(H.)M.A., Dimmeler A., Eberle B., et al. *Proc. SPIE*, **6738**, 67380O (2007).
4. Durécu A., Bourdon P., Fleury D., et al. *Proc. SPIE*, **8187**, 81870K (2011).
5. Santos C.N., Chrétien S., Merella L., et al. *Proc. SPIE*, **10797**, 107970S (2018).
6. Hueber N., Vincent D., Morin A., et al. *Proc. SPIE*, **7660**, 766042 (2010).
7. Goodman J.W. *Statistical Optics* (New York: Wiley-Interscience, 1985; Moscow: Mir, 1988).
8. Trishenkov M.A. *Fotopriemnye ustroistva i PZS. Obnaruzhenie slabykh opticheskikh signalov* (Photodetectors and CCDs. Detection of Weak Optical Signals) (Moscow: Radio i svyaz', 1992).
9. Voshchula I.V., Dlugunovich V.A., Zhumar' A.Yu. *Nauchno-Tekh. Vedom. SPbGPU. Ser. Fiz.-Mat. Nauki*, **182** (4), Pt. 1, 56 (2013).
10. Levin B.R. *Teoreticheskie osnovy statisticheskoi radiotekhniki* (Theoretical Foundations of Statistical Radio Engineering) (Moscow: Radio i svyaz', 1989).
11. Abakumova A.A., Malinova T.P., Medennikov P.A., Pavlov N.I. *Opt. Zh.*, **86** (8), 56 (2019).
12. Popov I.A. *Doct. Diss.* (St. Petersburg, SPbITMO, 2000).